

Acoustic Emission Monitoring of Damage Evaluation in Ceramics Submitted to Thermal Shock

F. Mignard, C. Olagnon & G. Fantozzi

Laboratoire GEMPPM, URA CNRS 341, bât. 502, INSA de Lyon, 20 bd. A. Einstein, 69621 Villeurbanne Cedex, France

(Received 27 September 1994; revised version received 3 February 1995; accepted 7 February 1995)

Abstract

In studies conducted on two ceramic materials, namely a porous alumina and a dense zirconia, it is shown that a simple acoustic emission experiment can provide valuable information on the processes of thermal shock degradation in the materials.

Acoustic emission technique for thermal shock damage evaluation of ceramics is particularly attractive because it is non-destructive and it gives *in-situ* information. However, the complexity of the acoustic emission (AE) response of a material makes the quantitative analysis difficult to achieve.¹ Konsztowicz^{2,3} used AE for detecting the damaging of refractory or high thermal shock resistance ceramics quenched in silicon oil, but he has not made any direct correlation between the acoustic emission activity and the number of cracks formed. He has also pointed out that not all the signals recorded could be directly related to strength degradation. AE was also used in rising thermal shock by laser irradiation in order to monitor the degradation of thermal barrier coating.⁴

The goal of this work is to show direct relations between AE and thermal shock degradation on relatively dense material, in order to use this technique for monitoring a thermal shock apparatus.

For this purpose thermal shock tests were conducted on two commercial ceramic materials, a coarse grain porous alumina (grade AL24, Degussa, Germany) and a magnesia partially stabilised zirconia (grade Z500, Morgan Matroc, UK). Thermal shock tests consisted of heating the specimens to various high temperatures and to cool them by jet air as described elsewhere.⁵ Acoustic emission response of the specimen was recorded with piezoelectric sensor (Bruel & Kjaer sensor, model 8313, resonance frequencies: 250 kHz) connected to a pre-amplifier (Bruel & Kjaer sensor, model 2637, fixed gain: 40 dB) and a main amplifier (Bruel & Kjaer sensor, model 2638, vari-

able gain: 20 dB chosen) leading to a total gain of 60 dB, as described by Peigné.⁶ The AE transducer is clamped at the end of a wave guide which plays also the role of a specimen holder (Fig. 1). The envelope of the AE signals delivered by the amplifier is sampled at a frequency of 10 kHz by means of digital/analogical converter driven by a micro-computer. Rectangular flexure specimens of dimensions $4 \times 6 \times 40$ mm³ were used. The specimens were cooled during 6 s at room temperature by 2 jet air nozzles. This cooling time was shown to be longer than the degradation duration. During the cooling, the acoustic emission was recorded. Alumina specimens were tested as ground and zirconia specimen were polished at 3 μ m. Special care regarding subeutectoid ageing treatment was accorded to enhance mechanical properties of Mg–PSZ and to remove residual stresses. The resistance to thermal shock was evaluated in terms of elastic modulus variations and retained strength as shown in Fig. 2. At a critical thermal shock temperature ΔT_c , both elastic modulus and retained strength decrease. The number of acoustic emission events is also reported in Fig. 2. Note that the apparition of the first acoustic emission event takes place for the critical thermal shock temperature. This suggests that the degradation is effectively correctly recorded and that it occurs by unstable crack propagation. The number of acoustic peaks increases linearly when increasing the severity of the thermal shock. The critical thermal shock temperature difference is found to be $\Delta T_c = 670^\circ\text{C}$ for Mg–PSZ and $\Delta T_c = 700^\circ\text{C}$ for alumina. Thermal, elastic and mechanical properties of these two materials are quite different but their combination leads to similar ΔT_c values. It is worth noting that the thermal shock behaviour of the alumina is quite different from that of the Mg–PSZ. After ΔT_c , the retained strength of the alumina material is about $0.5 \sigma_R$ which is higher than the $0.15 \sigma_R$ retained strength measured in Mg–PSZ. The elastic modulus

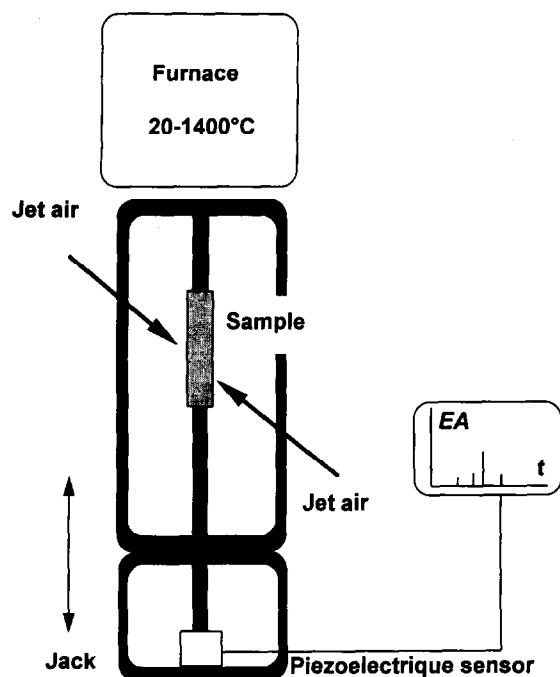


Fig. 1. Thermal shock device.

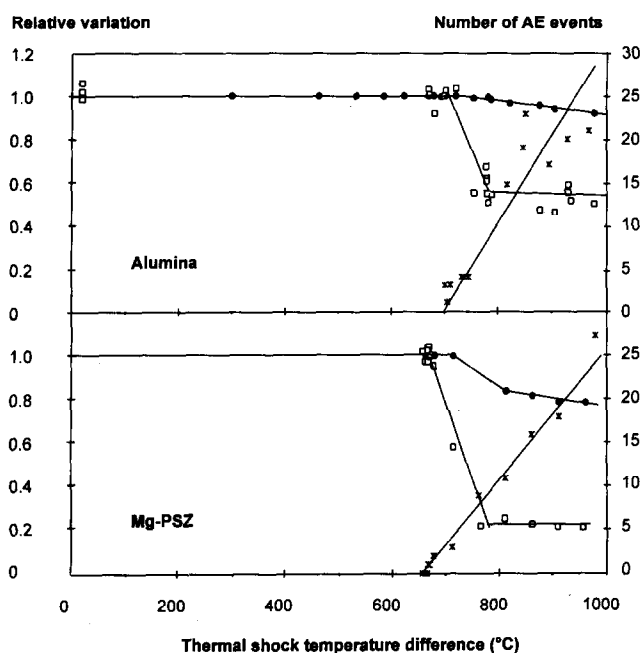
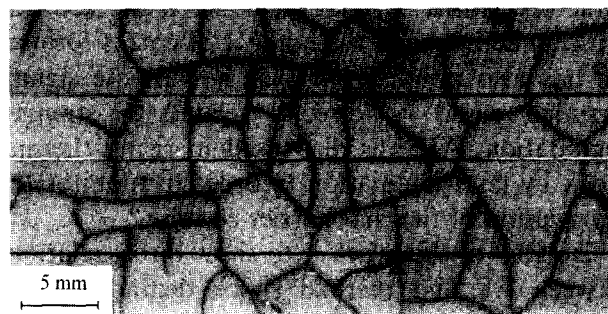


Fig. 2. Relative variation of retained strength (□), modulus of elasticity (●) and number of AE events (x) as a function of thermal shock temperature difference for alumina and Mg-PSZ materials.

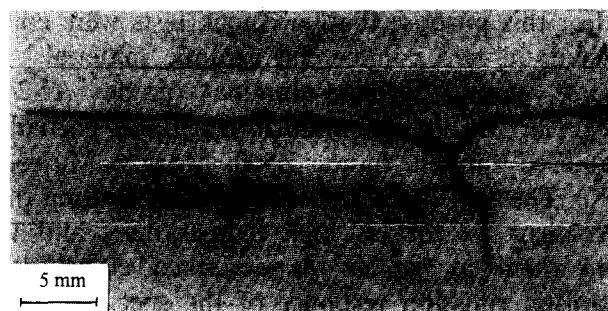
exhibits the same phenomena and its decrease with temperature is lower for the alumina than for the zirconia material. This means that the studied alumina behaves like a refractory material.

It is to be recalled that the thermal stress field is such that tensile stresses arise parallel to the surface, which leads to crack initiations from the surface. They could be easily observed by dye penetrant on the nearly dense zirconia material but the high amount of porosity in alumina material did not allow direct crack observation. In the

case of zirconia specimen the number of acoustic emission events could be correlated with the number of cracks at the surface of the body. The number of cracks induced by a thermal shock temperature near the critical temperature is low and easy to count. For higher thermal shock temperature differences the number of cracks strongly increases and the counting is difficult to achieve. Pictures were therefore taken from each side of the specimen and assembled together in order to represent a projection of the whole surface and to make the counting easier (see Figs 3(a) and (b)). The number of events in an acoustic emission response was counted with a computer treatment. The surface projection of a Mg-PSZ sample subjected to a thermal shock temperature of 714°C is represented in Fig. 3(a), and its associated acoustic emission response is represented in Fig. 4(a). Note that each crack corresponds to an AE peak. Figures 3(b) and 4(b) show the same phenomena but for a thermal shock temperature of 961°C leading to a higher crack density. Figure 5 shows the correlation between the number of cracks and the number of AE events for all the tested thermal shock temperatures. It appears clear that each crack propagation is associated to an AE peak; the error for the highest thermal shock temperature resulting from the way to count the cracks. This result suggests that the simple AE treatment conducted here can precisely enable us to record the degradation occurring during thermal shock. It might be especially useful for porous material



(a)



(b)

Fig. 3. (a) Damaged surface projection of a Mg-PSZ specimen for a thermal shock temperature difference of 714°C; (b) Damaged surface projection of a Mg-PSZ specimen for a thermal shock temperature difference of 961°C.

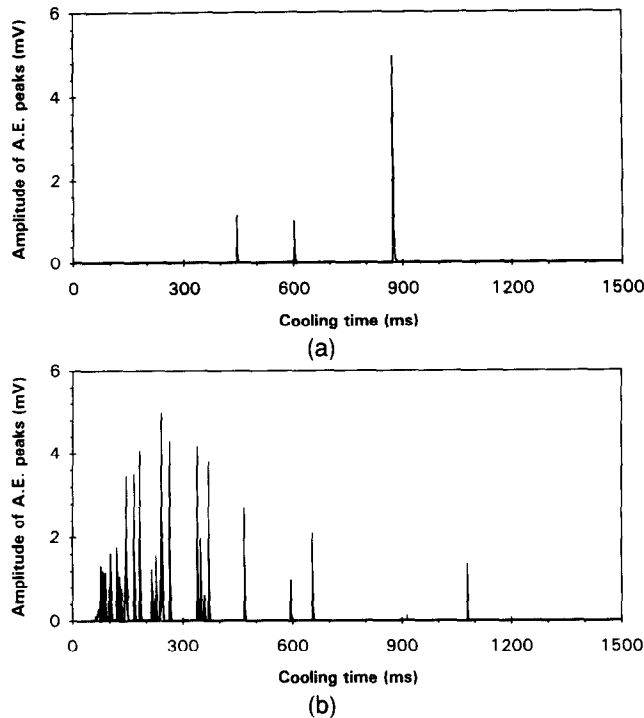


Fig. 4. (a) AE response of a Mg-PSZ specimen subjected to a thermal shock temperature difference of 714°C corresponding to the damaged surface shown in Fig. 3(a) (The amplitude is given in mV at the output of the sensor before the amplification of 60 dB); (b) AE response of a Mg-PSZ specimen subjected to a thermal shock temperature difference of 961°C corresponding to the damaged surface shown in Fig. 3(b) (The amplitude is given in mV the output of the sensor before the amplification of 60dB).

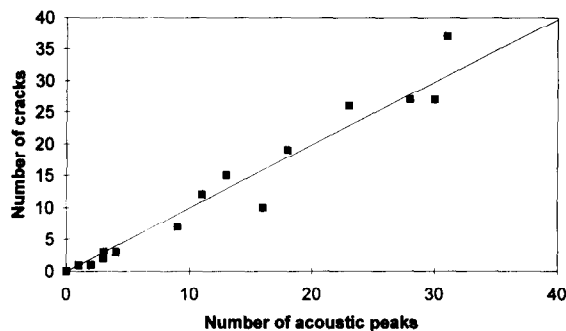


Fig. 5. Correlation between the number of AE peaks and the number of counted cracks in various Mg-PSZ specimens.

such as the alumina studied here and could also be extended to refractory materials.

It is also important to note that AE reflects particular cooling instants that can be associated to damage events. This is of major interest for such a transient problem where only final degradation is otherwise observed.

AE method which gives *in situ* information can be advantageously used for thermal fatigue where the cycling device can be automatically stopped from the apparition of an AE event.

Acknowledgement

The authors wish to acknowledge Dr R. Reza-khanlou and the 'Material Research Division' from Electricité de France (EDF) for their financial support and their interest in this work.

References

1. Ouanezard, N., Etude par émission acoustique de la résistance aux chocs et à la fatigue thermiques des matériaux céramiques, PhD thesis, Institut National des Sciences Appliquées de Lyon, Villeurbanne, France, 1983.
2. Konsztowicz, K. J., Crack growth and acoustic emission in ceramic during thermal shock, *J. Am. Ceram. Soc.*, **73**(3) 1990 502–8.
3. Konsztowicz, K. J., Acoustic emission amplitude analysis in crack growth studies during thermal shock of ceramics. In *Thermal shock and thermal fatigue behaviour of advanced ceramics*, ed. G. A. Schneider & G. Petzow, Kluwer Academic Publishers, The Netherlands, 1993 pp. 429–41.
4. Takahashi, H., Ishikawa, T., Okugawa, D. & Hashida, T., Laser and plasma-arc thermal shock/fatigue fracture evaluation procedure for functionally gradient materials, *ibid*, pp. 543–54.
5. Mignard, F., Olagnon, C., Fantozzi, Chantrenne, P., & Raynaud, M., *Thermal shock behaviour of a coarse grain alumina. Part I: Temperature field determination*, to be published.
6. Peigné, P., Résistance au chocs thermiques des céramiques thermomécaniques, PhD thesis, Institut National des Sciences Appliquées de Lyon, Villeurbanne, France, 1991.